Thin-film synthesis of metastable rocksalt $MgSnN_2$ without epitaxial stabilization

Kaede Makiuchi,[a,*] Fumio Kawamura,[b] Junjun Jia,[c] Hidenobu Murata,[d] Naoomi Yamada[a,*]

a. Department of Applied Chemistry, Chubu University, Aichi 487-8501, Japan.

b. Research Center for Materials Nanoarchitectonics, High-Pressure Structural Controls Group, National Institute for Materials Science, Ibaraki 305-0044, Japan.

c. Global Center for Science and Engineering, Waseda University, Tokyo 169-8555, Japan.

d. Department of Materials Science, Osaka Metropolitan University, Osaka 599-8531, Japan.

* Corresponding authors.

E-mail addresses: n-yamada@isc.chubu.ac.jp (N. Yamada), tk22013-8761@sti.chubu.ac.jp (K. Makiuchi).

ABSTRACT

Metastable rocksalt-type $MgSnN_2$ (rs-MTN) films were fabricated on amorphous substrates via the high-pressure heat treatment (HPHT) of wurtzite-type $MgSnN_2$ precursor layers. HPHT caused a wurtzite-to-rocksalt transition, and more importantly, the rocksalt structure was retained upon depressurization, even without epitaxial constraints from the substrates. Single-phase rs-MTN films were obtained over a limited range of pressures and temperatures using HPHT. A pressure–temperature diagram for HPHT was also constructed, and the transition enthalpy barrier was estimated to be 0.18–0.23 eV. These results provide essential information on the kinetics of the wurtzite-to-rocksalt transition of $MgSnN_2$.

Keywords: Rocksalt $MgSnN_2$, High-pressure heat treatment, wurtzite-to-rocksalt transition

1. Introduction

Ternary-nitride semiconductors have gained considerable attention over the past decade. In this context, a large stability map of the ternary nitrides was constructed using computational methods.[1] Among the ternary nitrides, II-IV-N_2 systems (II and IV represent divalent and tetravalent cations, respectively) have been intensively studied as candidates for optoelectronic materials because the II-IV-N_2 compounds usually adopt wurtzite (WZ)-derived structures and are structurally compatible with group-III nitrides.[2–4]

$MgSnN_2$ is a II-IV-N_2 compound, which takes on the WZ structure under ambient conditions (wz-MTN).[5–7] Recently, we identified a high-pressure phase in $MgSnN_2$,[8,9] although its presence was not previously predicted. The high-pressure phase adopts a cubic rocksalt (RS) structure with a disordered cation sublattice (rs-MTN) and a bandgap of 2.3 eV that makes it suitable for application as a top cell in tandem solar cells. Additionally, rs-MTN showed near-band-edge green-light emission in cathode luminescence measurements,[8,9] indicating that it is a direct-gap semiconductor. Thus, rs-MTN is an intriguing compound as an optoelectronic material; however, it has only been obtained in powder form to date. The development of a method to produce rs-MTN films is eagerly anticipated.

Recently, we developed a novel method for fabricating rs-MTN films using pressure-induced WZ-to-RS phase transition.[10] This method involves the high-pressure heat treatment (HPHT) of wz-MTN precursor films using a belt-type high-pressure apparatus. RS-type MgO single crystals were used as substrates to epitaxially stabilize the rs-MTN, thereby preventing its retransition to wz-MTN upon depressurization. HPHT at a temperature (T) of 700 °C under a pressure (P) of 6.5 GPa fully converted the wz-MTN precursors to rs-MTN films in 10 min, and the RS structure was retained even when depressurized. Nevertheless, it is not clear whether the use of a MgO substrate is indispensable. The fabrication of rs-MTN films on glass substrates for solar cell applications is desirable. In the previous study, HPHT was performed under only one condition above. Accordingly, the P–T region where single-phase rs-MTN films can be obtained remained unclear. Collectively, the use of HPHT to fabricate rs-

MTN films has not yet been established.

In this study, we performed HPHT on wz-MTN/glass at various pressures and temperatures, revealing that epitaxial stabilization is not necessary to obtain rs-MTN films. Furthermore, the results of the HPHT experiments reveal a transition enthalpy barrier.

2. Experiment

A wz-MTN precursor film was reactively sputtered from Mg and Sn targets on an alkali-free glass substrate heated at 400 °C. The wz-MTN specimen covered with another glass plate was charged into a high-pressure cell along with the NaCl pressure medium. Subsequently, HPHT was conducted at P = 4.5–7.7 GPa and T = 200–800 °C for 10 min (t_{HPHT}) using a belt-type high-pressure apparatus. Ex-situ X-ray diffraction measurements were conducted at room temperature using a diffractometer with Cu Kα radiation to investigate the crystalline phase. The details of the experimental conditions are provided in the Supplementary Material.

3. Results and discussion

As reported previously, the precursor films were in the WZ phase (Fig. 1a).[5–7] The wz-MTN precursors were always <001>-oriented. HPHT at P = 6.5 GPa and T = 700 °C fully converted the wz-MTN precursor to the RS phase (Fig. 1a), indicating that epitaxial stabilization is not necessary to obtain rs-MTN films by HPHT. The HPHT specimen could be recovered from high pressure without pulverization, as shown in the inset. The resulting rs-MTN films were oriented in the <100> direction. Therefore, HPHT converted the <001>-oriented wz-MTN films into <100>-oriented rs-MTN films. A molecular dynamics study of the pressure-induced WZ-to-RS transition of CdSe showed that the (001) plane of the WZ phase transformed into the (100) plane of the RS phase upon transition.[11] The same transformation likely occurred in the case of the MTN.

Fig. 1b shows a P–T diagram of the fraction of the RS phase (x). We define x as follows:

$$x = \frac{I_{RS200}}{I_{WZ002}+I_{RS200}}, \quad (1)$$

where I_{WZ002} and I_{RS200} denote the integral intensities of the WZ 002 and RS 200 diffraction peaks, respectively. Single-phase rs-MTN films (x = 1) were obtained in the region enclosed by the dotted line. At least $P \geq 6.5$ GPa was required to yield single-phase films. Increasing the T to 800 °C at 6.5 GPa resulted in the decomposition to metals such as Sn and Mg (Fig. S2, Supplementary Material). Such decomposition did not occur at 800 °C and P = 7.7 GPa because a higher P generally increases the decomposition temperature. Single-phase films can be obtained even at 600 °C when applying 7.7 GPa. Consequently, increasing P to 7.7 GPa extended the T range in which single-phase films can be obtained. The MTN films with x < 1 yielded in the relatively low T region at each P. The phase transition rate generally decreased with decreasing T. Meanwhile, the t_{HPHT} was only 10 min. Therefore, the transition was incomplete during this period. When t_{HPHT} was extended to 60 min at T = 500 °C and P = 6.5 GPa, the transition was almost completed ($x \approx 0.8$: Fig. 1c).

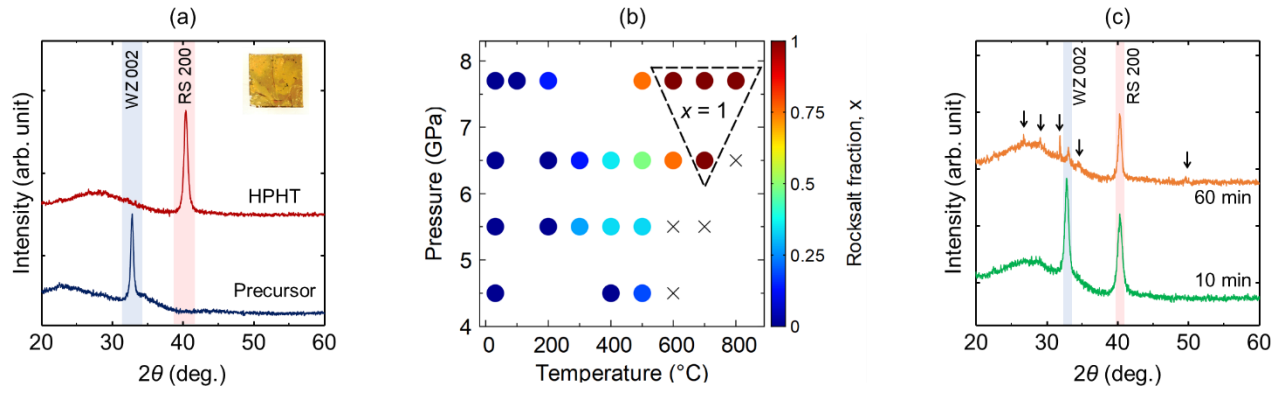

Fig. 1 (a) X-ray diffraction (XRD) patterns of precursor and HPHT films. HPHT was performed at P = 6.5 GPa and T = 700 °C. The inset shows the photograph of the HPHT specimen. (b) P–T diagram for rocksalt fraction after HPHT for 10 min. rs-MTN films with x = 1 were yielded in the region enclosed by the dashed triangle. The cross marks denote the decomposition. (c) XRD patterns of HPHT films treated at P = 6.5 GPa and T = 500 °C for 10 and 60 min. The peaks indicated by the arrows originate from the specimen holder.

The structural evolution of the MTN with T at P = 6.5 GPa is shown in Fig. 2a. The RS phase partially formed at T = 300 °C, and then became dominant phase with increasing T. Finally, the single-

phase rs-MTN was obtained at T = 700 °C. As seen from Fig. 2b, x exhibited Arrhenius-like behavior. Thus, nonlinear least-squares fitting of exponential function to the x vs. $1/(k_BT)$ data (k_B is the Boltzmann constant) for P = 6.5 and 7.7 GPa was performed to derive the enthalpy barrier (ΔH_B) for the WZ-to-RS transition. The best-fit curves were obtained at ΔH_B = 0.23 and 0.18 eV for P = 6.5 and 7.7 GPa, respectively. The ΔH_B value somewhat decreased with increasing P, which is consistent with the general tendency observed in the WZ-to-RS transition of AlN, GaN, and SiC (Fig. 3).[12]

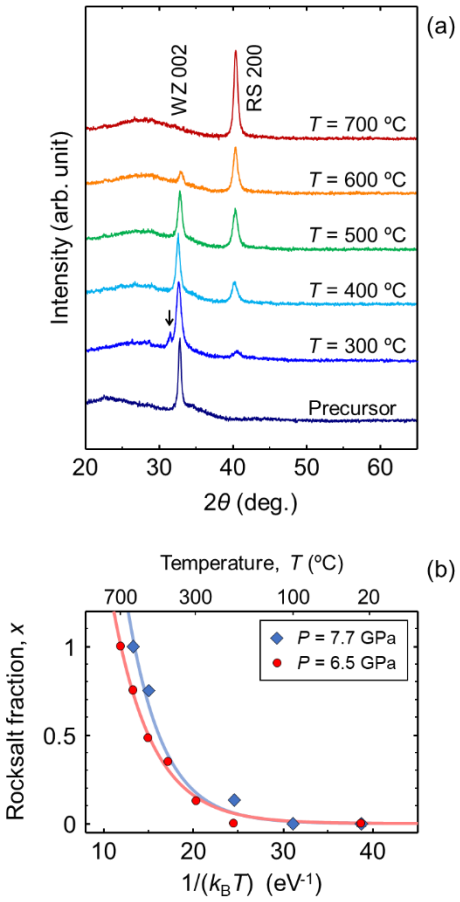

Fig. 2 (a) XRD patterns of high-pressure heat-treated films at different temperatures ranging from 300 to 700 °C under constant pressure (P = 6.5 GPa). The peak indicated by the arrow originates from the specimen holder. Heat-treatment temperature (T) dependence of the rocksalt fraction plotted with $1/(k_BT)$ (k_B denotes the Boltzmann constant). The solid curves are the best-fit exponential functions for the data for P = 6.5 and 7.7 GPa.

The ΔH_B of AlN, GaN, and SiC is known to have a similar value of approximately 0.25 eV at the equilibrium transition pressures.[12] Notably, the ΔH_B values obtained in this study were also similar to

this common value, as shown in Fig. 3. The equilibrium transition pressure for the MTN was estimated to be approximately 8 GPa based on first-principles calculations.[10] Since P = 6.5 and 7.7 GPa were similar to the equilibrium pressure, ΔH_B values similar to the common value were obtained.

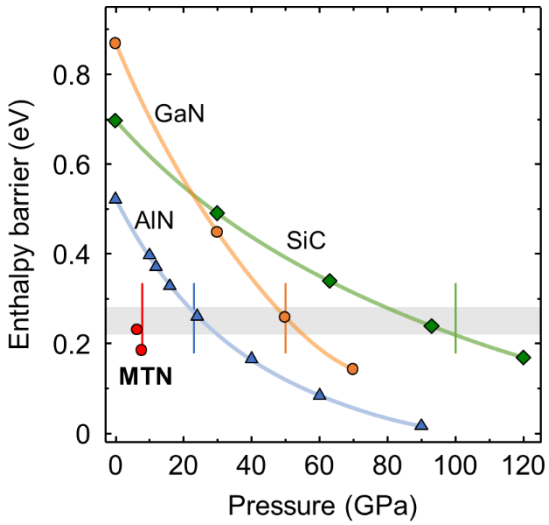

Fig. 3 Pressure-dependent enthalpy barriers of the wurtzite-to-rocksalt phase transformation for $MgSnN_2$ (MTN), AlN, GaN, and SiC. Vertical lines indicate the transformation pressures. The data for AlN, GaN, and SiC were previously published.[12] The transformation pressure for MTN is a previously published calculated value.[10] The gray area displays a rough estimation of the threshold enthalpy barrier at which the transformation occurs in AlN, GaN, and SiC.[12]

The rs-MTN films could not be subjected to optoelectronic measurements because many cracks were observed (Fig. S3, Supplementary Material). The crack formation was likely due to the volume shrinkage associated with the transition to the high-density RS phase and/or the difference in the thermal expansion coefficients between the glass substrate and the MTN. Crack formation is a problem that must be solved to investigate the optoelectronic properties of rs-MTNs.

4. Conclusions

We demonstrated that metastable rs-MTN films can be fabricated using HPHT without epitaxial constraints on the substrates. Single-phase rs-MTN films were yielded when HPHT was conducted at $T \geq 600$ °C and P = 7.7 GPa. The P–T diagram for the WZ-to-RS transition in MTN was also constructed,

and then the analysis of the T-dependence of x afforded an E_B (0.18–0.23 eV) close to the common value for AlN, GaN, and SiC. These findings will aid in the further study of the kinetics of the WZ-to-RS transition of the MTN.

Declaration of Competing Interest

The authors declare that they have no known competing financial interests or personal relationships that could have appeared to influence the work reported in this paper.

Acknowledgments

This study was supported by the NIMS Joint Research Hub Program.

References

1. W. Sun, C.J. Bartel, E. Arca, S.R. Bauers, B. Matthews, B. Orvañanos, B.-R. Chen, M.F. Toney, L.T. Schelhas, W. Tumas, J. Tate, A. Zakutayev, S. Lany, A.M. Holder, G.A. Ceder, Nat. Mater. 18 (2019) 732–739.
2. W.R.L. Lambrecht, A. Punya, Heterovalent ternary II–IV–N_2 compounds: perspectives for a new class of wide-band-gap Nitrides, in B. Gil (Ed.), III-nitride semiconductors and their modern devices, Oxford University Press, Oxford, 2013 pp. 519–585.
3. L. Lahourcade, N.C. Coronel, K.T. Delaney, S.K. Shukla, N.A. Spaldin, H.A. Atwater, Adv. Mater. 25 (2013) 2562–2566.
4. I.S. Khan, K.N. Heinselman, A. Zakutayev, J. Phys. Energy 2 (2020) 032007.
5. R.A. Makin, K. York, S.M. Durbin, N. Senabulya, J. Mathis, R. Clarke, N. Feldberg, P. Miska, C.M. Jones, Z. Deng, L. Williams, E. Kioupakis, R.J. Reeves, Phys. Rev. Lett. 122 (2019) 256403.
6. A.L. Greenaway, A.L. Loutris, K.N. Heinselman, C.L. Melamed, R.R. Schnepf, M.B. Telekamp, R. Woods-Robinson, R. Sherbondy, D. Bargett, S. Bauers, A. Zakutayev, S.T. Christensen, S. Lany, A.C. Tamboli, J. Am. Chem. Soc. 142 (2020) 8421–8430.
7. N. Yamada, K. Matsuura, M. Imura, H. Murata, F. Kawamura, ACS Appl. Electron. Mater. 3 (2021) 1341–1349.
8. F. Kawamura, M. Imura, H. Murata, N. Yamada, T. Taniguchi, Eur. J. Inorg. Chem. 2020 (2020) 446–451.
9. F. Kawamura, H. Murata, M. Imura, N. Yamada, T. Taniguchi, Inorg. Chem. 60 (2021) 1773–1779.
10. K. Makiuchi, F. Kawamura, J. Jia, Y. Song, S. Yata, H. Tampo, H. Murata, N. Yamada, Chem. Mater. 35 (2023) 2095–2106.
11. F. Shimojo, S. Kodiyalam, I. Ebbsjö, R.K. Kalia, A. Nakano, P. Vashishta, Phys. Rev. B 70 (2004) 184111.
12. S. Limpijumnong, S. Jungthawan, Phys. Rev. B 70 (2004) 054104.